A Novel Spatial Modulation Based on Cosine Function Pattern

Liyan Zhang[1], Wenbin Zhang[1,2(✉)], Jiaqi Su[1], and Shaochuan Wu[1]

[1] Harbin Institute of Technology, Harbin 150001, People's Republic of China
zwbgxy1973@hit.edu.cn
[2] Science and Technology on Communication Networks Laboratory, Shijiazhuang 050050, Hebei, People's Republic of China

Abstract. Spatial modulation (SM) is a special type of Massive MIMO technology, which utilizes the index of transmit antenna to carry some information bits. Recently, a novel spatial modulation called ABPM appears, which uses the index of antenna beam pattern to carry some information bits. When the receivers are located at the cross points of all beam patterns, ABPM is better than traditional spatial modulation in term of bit error rate (BER). However, the probability that receivers located at the position above is low. Thus ABPM can not be widely used in application. In order to solve this problem, this paper proposes a new method of beam pattern modulation based on cosine function pattern (M-CBPM), the scheme uses the Woodword-Lawson algorithm to calculate the weighted vectors and is more suitable for mobile communication scenarios. The results of theory analysis and simulation show that M-CBPM is better than traditional spatial modulation in term of BER and transmission rate.

Keywords: MIMO · Spatial modulation · Antenna beam pattern modulation · Massive MIMO · M-CBPM

1 Introduction

Massive MIMO is a key technology of 5G, which covers many techniques in application [1]. One of these techniques is spatial modulation (SM), which has many advantages such as simple transmitter structure, low power consumption with few activated RF chains [2,3]. Thus, spatial modulation gradually becomes one of the technologies that attracts much attention in Massive MIMO area. According to the number of activated antennas, spatial modulation is classified into traditional SM and general SM, which activates one antenna and many antennas respectively [4–6].

Recently, a novel SM called Antenna Beam Pattern Modulation (ABPM) is proposed [7], which transmits a part of information bits by generating the pattern

Supported by National Nature Science Foundation of China (NSFC) under Grant 62071148.

Q. Guo et al. (Eds.): WiSATS 2021, LNICST 410, pp. 405–417, 2022.
https://doi.org/10.1007/978-3-030-93398-2_39

of antenna array. In the receiving part, the maximum likelihood(ML) algorithm is used to recover the transmitted bits. The ML algorithm brings the best BER performance to the receiver, but results in the highest computational complexity. To tackle with this problem, [8] used lattice reduction and linear detection jointly. This receiver structure reduces the computational complexity efficiently, at the same time, achieving the same BER performance as ML algorithm.

In ABPM, there are a lot of available patterns of antenna array. If one receiver lies in the non-intersection area among different patterns, it can not receive the electromagnetic wave from certain patterns, which results in some not recognized patterns in this receiver. To solve this intrinsic problem of ABPM, this paper proposes a scheme based on cosine pattern of antenna array.

The contents of this paper are organized as follows. First, we introduce the model of ABPM including transmitter, wireless channel and receiver. Second, we propose modified cosine beam pattern modulation, which makes receivers can identify each beam pattern anywhere. Third, we give numerical results of our scheme to show each factor's effect on BER and spectral efficiency. At last, the conclusion is drawn.

Notation: $\mathbf{A}^{\mathrm{T}}$, $\mathbf{A}^{\mathrm{H}}$ and a^* represent the transpose, the conjugate transpose and the conjugate respectively.

2 The Model of ABPM

The model of ABPM is shown in Fig. 1, which includes transmitter, wireless channel and receiver. At the transmitter, the input bit stream is divided into many groups, each group includes k bits which can be expressed as $\mathbf{b} = [\, b_1 \; b_2 \; \cdots \; b_k \,]$. Next, we convert each bit-group into two parts by serial-to-parallel conversion. The first m bits are divided into the first part, which are used to select a weighted vector of transmit antenna by some mapping relationship. The weighted vector can be expressed as $\mathbf{w} = \{w_1, w_2, \cdots w_{N_t}\}$, where N_t is the number of transmit antennas. The next $k - m$ bits are divided into the second part, these bits are mapped to many points of constellation graph according to the modulation type. The constellation point collection can be expressed as s. Then, multiplying the selected weighted vector w by the selected constellation point collection s, we can obtain the transmission vector $\mathbf{x} = \mathbf{w} \cdot \mathbf{s} = \left[x_1 \; x_2 \; \cdots \; x_{N_t} \right]^{\mathrm{T}}$ This vector will be transmitted to wireless channel described by a $N_t \times N_r$ matrix $\mathbf{H}$, whose arbitrary element $H_{i,j}, i \in \{1, 2, \cdots N_t\}, j \in \{1, 2, \cdots N_r\}$ follows the i.i.d circular symmetry complex Gaussian distribution with $\mathcal{CN}(0, 1)$. After transmission, the signal vector arriving at receiving antenna array can be expressed as $\mathbf{y} = \mathbf{H}\mathbf{x} + \mathbf{v}$, where $\mathbf{v} = \left[v_1 \; v_2 \; \cdots \; v_{N_r} \right]^{\mathrm{T}}$ is the additive white Gaussian noise (AWGN) vector introduced by receiving antennas. The elements of $\mathbf{v}$ follow the i.i.d complex Gaussian distribution with $\mathcal{CN}\left(0, \sigma_v^2\right)$. Assuming that the channel is quasi-static, that is, the elements of $\mathbf{H}$ do not change during the transmission of $\mathbf{b}$, and $\mathbf{H}$ in different transmission during are independent. At the receiver, we use maximum likelihood (ML) algorithm to detect the transmitted k bits from $\mathbf{y}$.

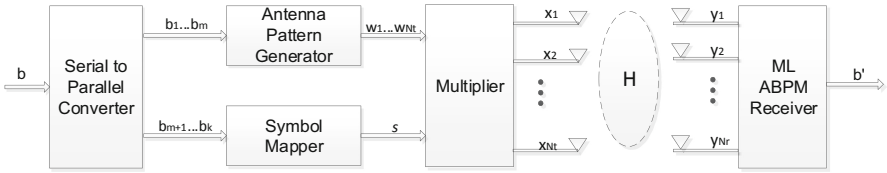

Fig. 1. The model of ABPM system.

In order to understand the principle of ABPM, we take a 2×2 MIMO system as an example. Each group of bits $\mathbf{b} = [b_1\ b_2\ b_3]$ includes three information bits, the first bit b_1 is used to select a weighted vector w , the next two bits b_2, b_3 are mapped to a constellation point of QPSK. The weighted vector w is determined by

$$w_1^{\mathrm{H}}\left[\mathbf{a}\left(120^\circ\right)\mathbf{a}\left(60^\circ\right)\right]^{\mathrm{H}} = \left[1\ 0\right]^{\mathrm{T}} \tag{1}$$

$$w_2^{\mathrm{H}}\left[\mathbf{a}\left(60^\circ\right)\mathbf{a}\left(120^\circ\right)\right]^{\mathrm{H}} = \left[1\ 0\right]^{\mathrm{T}} \tag{2}$$

Where, $\mathbf{a}\left(120^\circ\right) = \left[1\ e^{-j2\pi d\cos(120^\circ)/\lambda}\right]$ and $\mathbf{a}\left(60^\circ\right) = \left[1\ e^{-j2\pi d\cos(60^\circ)/\lambda}\right]$ are array response vectors at 120° and 60° respectively. When $b_1 = 0$, the beam pattern 1 is selected, the gain of this pattern at 120° is 1, and the gain at 60° is 0. When $b_1 = 1$, the beam pattern 2 is selected, the gain of this pattern at 60° is 1, and the gain at 120° is 0. Generally, d is the distance between adjacent antenna elements of array, which is equal to $\lambda/2$. λ is the wavelength. After solving the w_1 and w_2, two beam patterns corresponding to them can be drawn in Fig. 2. Obviously, there is large difference between two beam patterns. If the receiver can discriminate them, it will recovery one bit information correctly. However, if the receiver locates at the red point in Fig. 2, it can not receive the signal carried by beam pattern 2. This is an intrinsic weak point of ABPM. In this paper, our proposed scheme can solve this problem efficiently.

3 Modified Cosine Beam Pattern Method (M-CBPM)

Considering one cell in cellular network, where a base station is located in the center of circular area and some user equipment are uniformly located near the base station. First, in Fig. 3, we divide the circle into n sectors equally and allocate different frequencies to different sectors. Thus, there are no interference among different sectors. The base station has many antenna arrays, each of them is allocated to one sector. The desired beam pattern is described by the following cosine function.

$$\begin{gathered} p\{\xi\} : F(\theta,\xi) = \left|\cos\left[\left(\Omega_0 + \xi\cdot\Delta\omega\right)(\theta-\alpha)\right]\right|, \xi = 1,2,\cdots 2^m, \theta\in[0,\pi] \\ \Omega_0 + 2^m\cdot\Delta\omega = \Omega_m \end{gathered} \tag{3}$$

Where, α stands for the central angle of a sector, m represents the number of bits used to select weighted vector, in other words, there are 2^m weighted

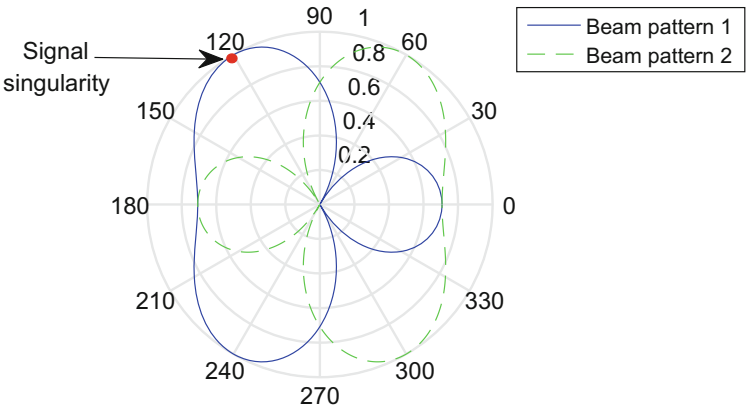

Fig. 2. Two beam patterns corresponding to w_1 and w_2. (Color figure online)

vectors available. Ω_m is the maximum cosine angular frequency that can be synthesized by N_t transmit antennas, it is equal to $N_t/2\pi$ by spatial sampling theory and determines the narrowest width of main lobe $\theta_{\min} = \left(2\arccos\left(\frac{\sqrt{2}}{2}\right)\right)/\Omega_m$. Thus, the number of sectors n is equal to $n = \pi/\theta_{\min}$. When m, $\Delta\omega$ and Ω_m are fixed, as an additional angle frequency, Ω_0 ensures $\Omega_0 + 2^m\Delta\omega = \Omega_m$. Figure 4 is an example of cosine pattern with $m = 3$and $\alpha = \pi/2$. By observing (3), we can find that when Ω_m is fixed, $\Delta\omega$ determines the similar degree among beam patterns, which reduces with the increase of $\Delta\omega$. So the receiver can identify different patterns more easily and the system has a better BER performance. It is worth noting that when Ω_m is fixed, the increase of $\Delta\omega$ also results in the reduction of m, which means the reduction of number of information bits carried by beam pattern.

Next, we will design the weighted vectors corresponding to the cosine beam patterns. Obviously, we can not utilize method introduced in (1) and (2) to calculate the weighted vectors. Here, we introduce Woodword-Lawson algorithm [9] to calculate the weighted vectors from a desired cosine beam pattern. First, we supply basic principle of this algorithm. Taking the central point of axis of uniform linear array as a reference point, the response vector of a uniform linear array can be written as

$$\begin{aligned}\mathbf{v}(\theta) = \Big[& e^{j\left(0-\frac{N_t-1}{2}\right)\frac{2\pi d\cos\theta}{\lambda}} \; e^{j\left(1-\frac{N_t-1}{2}\right)\frac{2\pi d\cos\theta}{\lambda}} \; \cdots \\ & e^{j\left(N_t-2-\frac{N_t-1}{2}\right)\frac{2\pi d\cos\theta}{\lambda}} \; e^{j\left(N_t-1-\frac{N_t-1}{2}\right)\frac{2\pi d\cos\theta}{\lambda}} \Big]^{\mathrm{T}}\end{aligned} \tag{4}$$

Where, λ is the wavelength of electric-magnetic wave. N_t is the number of transmit antennas, without loss of generality, we assume it is an odd. d is the distance between adjacent antennas, generally speaking, $d = \lambda/2$. θ is the angle between

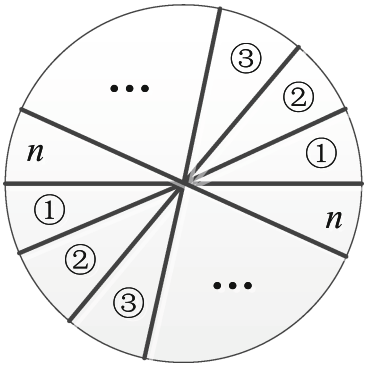

Fig. 3. The cell is divided into n sectors equally.

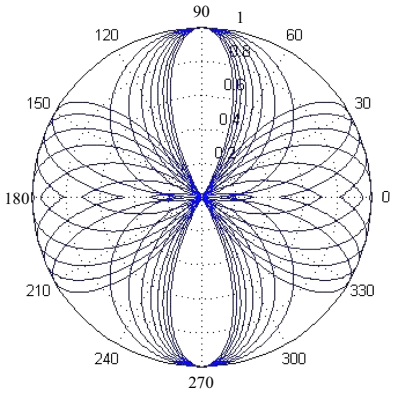

Fig. 4. Beam pattern set with $m = 3$ and $\alpha = \pi/2$.

direction of electric-magnetic wave and axis of array. Thus, the pattern of uniform linear array with N antenna elements can be written as

$$F(\theta) = \mathbf{w}^H \mathbf{v}(\theta) = \sum_{n=0}^{N_t-1} w_n^* e^{j\left(n-\frac{N_t-1}{2}\right)\pi\cos\theta} \tag{5}$$

We use the following sampling function to fit the pattern of (5).

$$\frac{\sin\left[N_t\pi(\cos\theta-\cos\theta_m)/2\right]}{N\sin\left[\pi(\cos\theta-\cos\theta_m)/2\right]}, 0 \le \theta \le \pi \tag{6}$$

Where, θ_m denotes the m-th sampling angle, the sampling is uniformly, which means $\cos\theta_{m+1} - \cos\theta_m = 2/N_t$, $\forall m \in \{0, 1, 2, \cdots N_t - 1\}$. Therefore, the pattern in (5) can be rewritten as

$$F(\theta) = \sum_{m=0}^{N_t-1} F_D(\theta_m) \frac{\sin\left[N_t\pi(\cos\theta-\cos\theta_m)/2\right]}{N_t\sin\left[\pi(\cos\theta-\cos\theta_m)/2\right]} \tag{7}$$

Where, $F_D(\theta_m)$ stands for the discrete pattern value on sampling point θ_m. Assuming that sampling points are symmetry about $\cos\theta = 0$. According to the sampling criterion of space, which is similar to time-frequency one, sampling interval equals $2/N_t$ in term of $\cos\theta$. So, the sampling angle must meet the following condition.

$$\cos\theta_m = \frac{2}{N_t}\left(m - \frac{N_t-1}{2}\right), m = 0, 1, \cdots, N_t - 1 \tag{8}$$

Next, we derive the expression of weighted vector from (7) utilizing $\sin x = (e^{jx} - e^{-jx})/2j$ and $\sum_{k=0}^{N_t-1} x^k = \frac{1-x^N}{1-x}$, we can rewrite (7) as

$$\begin{aligned}
F(\theta) &= \sum_{m=0}^{N_t-1} F_D(\theta_m)\frac{1}{N_t}\cdot\frac{e^{j\frac{N_t}{2}\pi(\cos\theta-\cos\theta_m)} - e^{-j\frac{N_t}{2}\pi(\cos\theta-\cos\theta_m)}}{e^{-j\frac{\pi}{2}(\cos\theta-\cos\theta_m)} - e^{-j\frac{\pi}{2}(\cos\theta-\cos\theta_m)}} \\
&= \sum_{m=0}^{N_t-1} F_D(\theta_m)\frac{1}{N_t}\cdot\frac{-e^{-j\frac{N_t}{2}\pi(\cos\theta-\cos\theta_m)}}{-e^{-j\frac{\pi}{2}(\cos\theta-\cos\theta_m)}}\cdot\left[\frac{1-e^{jN_t\pi(\cos\theta-\cos\theta_m)}}{1-e^{j\pi(\cos\theta-\cos\theta_m)}}\right] \\
&= \sum_{m=0}^{N_t-1} F_D(\theta_m)\frac{1}{N_t}\cdot e^{-j\frac{N_t-1}{2}\pi(\cos\theta-\cos\theta_m)}\cdot\sum_{k=0}^{N_t-1} e^{jk\pi(\cos\theta-\cos\theta_m)} \\
&= \sum_{m=0}^{N_t-1} F_D(\theta_m)\frac{1}{N_t}\cdot\sum_{k=0}^{N_t-1} e^{j\left(k-\frac{N_t-1}{2}\right)\pi(\cos\theta-\cos\theta_m)} \\
&= \sum_{k=0}^{N_t-1} e^{j\left(k-\frac{N_t-1}{2}\right)\pi\cos\theta}\left(\sum_{m=0}^{N_t-1} F_D(\theta_m)\frac{1}{N_t}\cdot e^{-j\left(k-\frac{N_t-1}{2}\right)\pi\cos\theta_m}\right) \qquad (9)
\end{aligned}$$

Comparing (5) with (9), we can obtain the k-th element of weighted vector.

$$w_k^* = \frac{1}{N_t}\sum_{m=0}^{N_t-1} F_D(\theta_m)\cdot e^{-j\left(k-\frac{N_t-1}{2}\right)\pi\cos\theta_m}, k = 0, 1, \cdots, N_t - 1 \qquad (10)$$

Now, we have derived the weighted vectors of general array pattern. Subsequently, we propose an algorithm to obtain the weighted vector based on cosine beam pattern.

Algorithm 1. Weighted vector calculation Algorithm for M-CBPM

Input: The number of transmit antennas N_t.
Output: The weighted vector $\mathbf{w}^H$.

1: Substituting N_t into (8), and calculating the sampling point θ_m;
2: Calculating $F_D(\theta_m)$ according to the desired pattern (3) and sampling point θ_m;
3: Substituting θ_m, N_t and $F_D(\theta_m)$ into (7), and synthesizing actual pattern $F(\theta)$;
4: Substituting θ_m, N_t and $F_D(\theta_m)$ into (10), and calculating the weighted vector $\mathbf{w}^H$;
5: **return** The weighted vector $\mathbf{w}^H$.

4 Performance Analysis of M-CBPM

First, we analyze the number of bits carried by weighted vectors in M-CBPM. We have known $\Omega_0 + 2^m\Delta\omega = \Omega_m$ and $\Omega_m = N_t/2\pi$. Once Ω_m and $\Delta\omega$ are determined, m can be maximized when $\Omega_0 = 0$. Thus, the weighted vectors can

carry $\log_2(\Omega_m/\Delta\omega)$ bits. Second, we analyze the BER performance of M-CBPM in theory. Without loss of generality, we select maximize likelihood(ML) to detect the received signal. Considering there are innumerable pattern schemes, we only analyze the up-bound of BER. Assuming that transmitter sends $\mathbf{x}_m$, and receiver judge $\mathbf{x}_{\hat{m}}$ by ML. The pairwise error probability (PEP) between $\mathbf{x}_m$ and $\mathbf{x}_{\hat{m}}$ can be written as

$$\begin{aligned} P\left(\mathbf{x}_m \to \mathbf{x}_{\hat{m}}\right) &= p\left(\left\|\mathbf{y}-\mathbf{H}\mathbf{x}_{\hat{m}}\right\|^2 - \left\|\mathbf{y}-\mathbf{H}\mathbf{x}_m\right\|^2 \le 0\right) \\ &= \mathbb{E}\left[Q\left(\sqrt{\frac{1}{2\sigma_v^2}\sum_m\sum_{\hat{m}}\left\|\mathbf{H}\left(\mathbf{x}_m-\mathbf{x}_{\hat{m}}\right)\right\|^2}\right)\right] \end{aligned} \tag{11}$$

Utilizing the union-bounding technique given by [10], the union bound on BER of M-CBPM can be written as

$$\begin{aligned} P_{e,bit} &\le \mathbb{E}_{\mathbf{x}_m}\left[\sum_{\hat{m}} N(m,\hat{m}) P\left(\mathbf{x}_m \to \mathbf{x}_{\hat{m}}\right)\right] \\ &\le \sum_{m}^{L}\sum_{\hat{m},\hat{m}\neq m}^{L} \frac{N(m,\hat{m})}{kL} P(\mathbf{x}_m \to \mathbf{x}_{\hat{m}}) \end{aligned} \tag{12}$$

Where, k denotes the number of information bits carried by each transmitted symbol of M-CBPM. L denotes the number of transmitted symbols of M-CBPM. $N(m,\hat{m})$ represents the number of different bits between $\mathbf{x}_m$ and $\mathbf{x}_{\hat{m}}$. $\mathbb{E}_{\mathbf{x}_m}$ stands for the expectation on $\mathbf{x}_m$. According to [10], $P\left(\mathbf{x}_m \to \mathbf{x}_{\hat{m}}\right)$ is given by

$$P\left(\mathbf{x}_m \to \mathbf{x}_{\hat{m}}\right) = \left(\frac{1-\frac{1}{p}}{2}\right)^{\Lambda}\sum_{q=0}^{\Lambda-1} 2^{-q}\binom{\Lambda-1+q}{q}\left(1+\frac{1}{p}\right)^q \tag{13}$$

Where, $p = \sqrt{1+1/E_s d^2(m,\hat{m})/4N_t\sigma_v^2}$, E_s is the average energy of symbols of M-CBPM, $\Lambda = N_t N_r$, σ_v^2 is the variance of AWGN, $d(m,\hat{m})$ is the Euclidean distance between $\mathbf{x}_m$ and $\mathbf{x}_{\hat{m}}$. Substituting (13) into (12) and deriving the up-bound of BER of M-CBPM.

$$P_{e,bit} \le \sum_{m}^{L}\sum_{\hat{m},\hat{m}\neq m}^{L} \frac{N(m,\hat{m})}{kL}\left(\frac{1-\frac{1}{p}}{2}\right)^{\Lambda}\sum_{q=0}^{\Lambda-1} 2^{-q}\binom{\Lambda-1+q}{q}\left(1+\frac{1}{p}\right)^q \tag{14}$$

Observing the above expression of p, we find that $p \ge 1$. If $p = 1$, the result of (14) is zero. If $p \neq 1$, the smaller p is benefit to the BER of M-CBPM. So it is expected that the Euclidean distance between $\mathbf{x}_m$ and $\mathbf{x}_{\hat{m}}$ is as possible as large. Next, we analyze the effect of $\Delta\omega$ on the Euclidean distance between $\mathbf{x}_m$ and $\mathbf{x}_{\hat{m}}$. Assuming $\mathbf{x}_m = \mathbf{w}_m s_m$ and $\mathbf{x}_{\hat{m}} = \mathbf{w}_{\hat{m}} s_{\hat{m}}$. The event $\mathbf{x}_m \neq \mathbf{x}_{\hat{m}}$ happens when any one of the following three conditions holds, which are $\mathbf{w}_m = \mathbf{w}_{\hat{m}}, s_m \neq s_{\hat{m}}$, $\mathbf{w}_m \neq \mathbf{w}_{\hat{m}}, s_m = s_{\hat{m}}$ and $\mathbf{w}_m \neq \mathbf{w}_{\hat{m}}, s_m \neq s_{\hat{m}}$. Our analyses do not involve in any

condition. For simplicity, assuming $|s_m|^2 = |s_{\hat{m}}|^2 = c$. The squared Euclidean distance between $\mathbf{x}_m$ and $\mathbf{x}_{\hat{m}}$ is written as

$$\begin{aligned}
d^2(m,\hat{m}) &= \|\mathbf{w}_m s_m - \mathbf{w}_{\hat{m}} s_{\hat{m}}\|^2 \\
&= \sum_{n=1}^{N_t} \left[(w_{m,n} s_m - w_{\hat{m},n} s_{\hat{m}}) \cdot (w_{m,n} s_m - w_{\hat{m},n} s_{\hat{m}})^*\right] \\
&= \sum_{n=1}^{N_t} \left[w_{m,n} s_m w_{m,n}^* s_m^* + w_{\hat{m},n} s_{\hat{m}} w_{\hat{m},n}^* s_{\hat{m}}^* - (w_{\hat{m},n} s_{\hat{m}} w_{m,n}^* s_m^* + w_{m,n} s_m w_{\hat{m},n}^* s_{\hat{m}}^*)\right] \\
&= \sum_{n=1}^{N_t} \left[|w_{m,n}|^2 c + |w_{\hat{m},n}|^2 c - (w_{\hat{m},n} w_{m,n}^* s_{\hat{m}} s_m^* + w_{m,n} w_{\hat{m},n}^* s_m s_{\hat{m}}^*)\right] \\
&\geq \sum_{n=1}^{N_t} \left[c|w_{m,n}|^2 + c|w_{\hat{m},n}|^2 - c(w_{\hat{m},n} w_{m,n}^* + w_{m,n} w_{\hat{m},n}^*)\right] \\
&\geq c \sum_{n=1}^{N_t} \|w_{m,n} - w_{\hat{m},n}\|^2 \\
&\geq c\|\mathbf{w}_m - \mathbf{w}_{\hat{m}}\|^2 = c d^2(\mathbf{w}_m, \mathbf{w}_{\hat{m}})
\end{aligned} \tag{15}$$

From (15), we can find that the Euclidean distance between $\mathbf{x}_m$ and $\mathbf{x}_{\hat{m}}$ depends on the Euclidean distance between $\mathbf{w}_m$ and $\mathbf{w}_{\hat{m}}$. According to the expression of the weighted vectors in (10), we can rewrite the $d(\mathbf{w}_m, \mathbf{w}_{\hat{m}})$ as

$$\begin{aligned}
d(\mathbf{w}_m, \mathbf{w}_{\hat{m}}) &= \left(\sum_{n=1}^{N_t} |w_{m,n} - w_{\hat{m},n}|^2\right)^{\frac{1}{2}} \\
&= \left(\sum_{n=1}^{N_t} \left(\sum_{h=0}^{N_t-1} \left(\left(F_m(\theta_h) - F_{\hat{m}}(\theta_h)\right) e^{-j\left(n-\frac{N_t-1}{2}\right)\pi\cos\theta_h}\right) \cdot \right.\right. \\
&\quad \left.\left. \left(\left(F_m(\theta_h) - F_{\hat{m}}(\theta_h)\right) e^{-j\left(n-\frac{N_t-1}{2}\right)\pi\cos\theta_h}\right)^* \right)\right)^{\frac{1}{2}}
\end{aligned} \tag{16}$$

Substitute (3) into $F_m(\theta_h) - F_{\hat{m}}(\theta_h)$ and obtain

$$F_m(\theta_h) - F_{\hat{m}}(\theta_h) = \cos\left[m \cdot \Delta\omega(\theta_h - \alpha)\right] - \cos\left[\hat{m} \cdot \Delta\omega(\theta_h - \alpha)\right], \theta_h \in [0, \pi] \tag{17}$$

From (3), we have known that the larger $\Delta\omega$ is, the less the number of weighted vectors available is. It means that the average distance between $m \cdot \Delta\omega$ and $\hat{m} \cdot \Delta\omega$ becomes larger with the increase of $\Delta\omega$. Consequently, $F_m(\theta_h) - F_{\hat{m}}(\theta_h)$ in (17) increases in average meaning, and $d(\mathbf{w}_m, \mathbf{w}_{\hat{m}})$ in (16) also increases.

5 Numerical Results

Due to $\Omega_m = N_t/2\pi$, the number of information bits carried by each M-CBPM symbol is $\log_2\left[N_t/\left(2\pi\Delta\omega\right)\right]$. However, the number of information bits carried by

each ABPM symbol is $\log_2 N_t$. So the actual number of transmitted information bits carried by M-CBPM symbol depends on $\Delta\omega$. In order to show the effect of $\Delta\omega$ clearly, the Fig. 5 is drawn, which shows the comparison of the results of SM and M-CBPM with different $\Delta\omega$. By observing the fig, we can see that once $\Delta\omega \geq 0.001$, M-CBPM excels SM in term of the number of information bits carried by each transmitted symbol. Whether it is SM or M-CBPM, the number of information bits carried by each symbol increases with the number of transmit antennas. Next, we show the effect of $\Delta\omega$ on BER of M-CBPM.

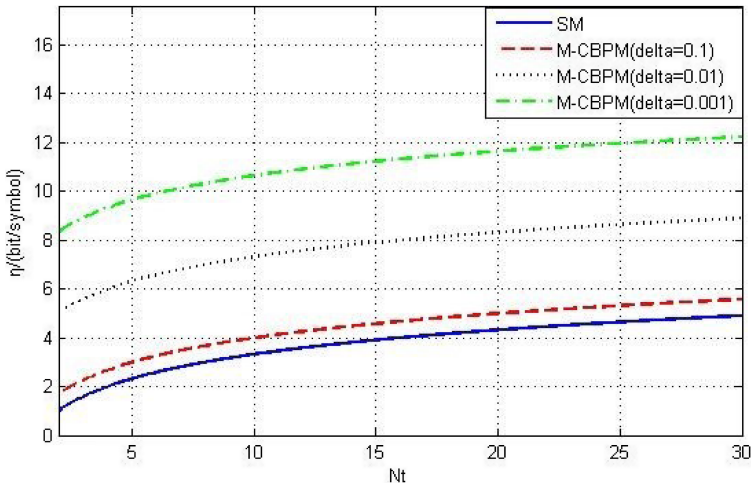

Fig. 5. Under the condition of different $\Delta\omega$, the number of information bits carried by each symbol varies with the number of transmit antennas.

First, we set the system parameters in the simulation and list them in Table 1. The receiver uses maximize likelihood algorithm to detect the received signal, and Fig. 6 shows the curves of BER with different m. By observing this fig, we can find that when the SNR is low, m has little effect on BER. However, with the increase of m, the number of information bits carried by each transmitted symbol increases. Subsequently, the number of transmitted pattern increases, which leads to the increase of transmit antennas according to the space sampling theory. Therefore, there is a trade-off between the number of transmit antennas and transmission rate. It is lucky that there are a very large number of transmit antennas in massive MIMO system, which ensures both reliability and validity of transmission.

Table 1. System parameters in simulation.

Parameter of system	Value
The number of transmit antennas N_t	25
The number of receive antennas N_r	5
Wavelength of the carrier	0.116 m
The distance between adjacent antennas in ULA	0.058 m
Ω	3
$\Delta\omega$	0.3

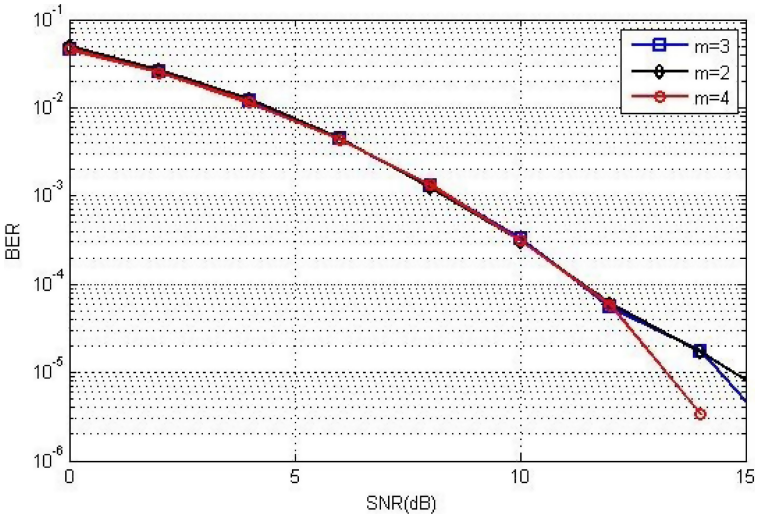

Fig. 6. The BER performance of M-CBPM with different m.

We have known that $\Delta\omega$ has an effect on the Euclidean distance between weighted vectors. The larger the $\Delta\omega$, the smaller the correlation between beam patterns. Therefore, the receiver can distinguish different patterns more easily, and the BER performance of the receiver can be improved. To validate the conclusion above, we implement the simulation of BER on different $\Delta\omega$, the simulation results are shown in Fig. 7. From this fig, we can see that the BER performance of M-CBPM improves efficiently with the increase of $\Delta\omega$.

In order to show the effect of Woodword-Lawson algorithm, we give the beam patterns with different $\Delta\omega$ in Fig. 8. These patterns are synthesized by this algorithm. Comparing this fig with Fig. 4, we find that the pattern synthesized by Woodword-Lawson algorithm is close to the ideal pattern.

The simulations above are based on maximize likelihood algorithm, which is known to have the best BER performance. However, the computational complexity is the highest. In order to obtain the trade-off between the BER and complexity, we implement the simulation about MMSE algorithm, and the results of simulation are shown in Fig. 9.

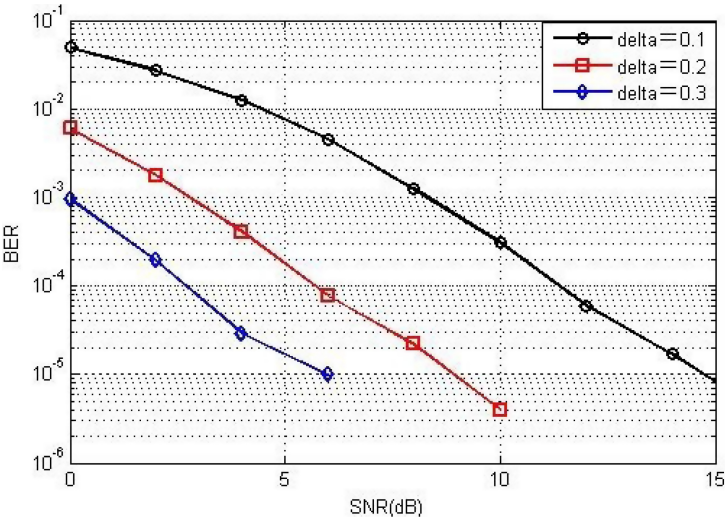

Fig. 7. The BER performance of M-CBPM with different $\Delta\omega$.

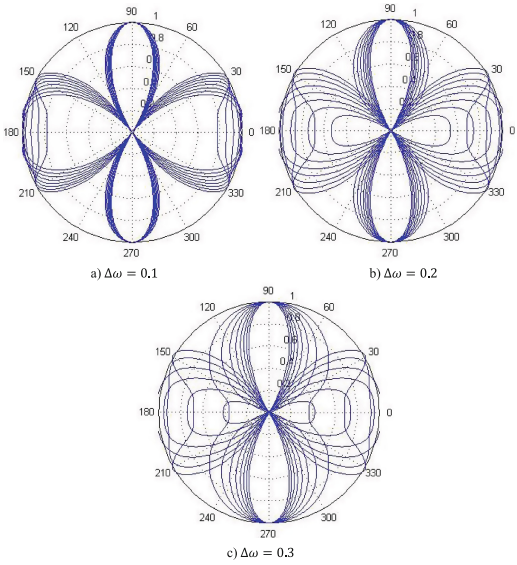

Fig. 8. The pattern synthesized by Woodword-Lawson algorithm with different $\Delta\omega$.

By observing this fig, we can find that although ML is better than MMSE in term of BER, as SNR increase, the BER performance of MMSE with different N_r will gradually improve, especially for the larger N_r. If the requirement for the BER of the receiver is not high, the MMSE algorithm with a large number of receive antennas is a suitable choice.

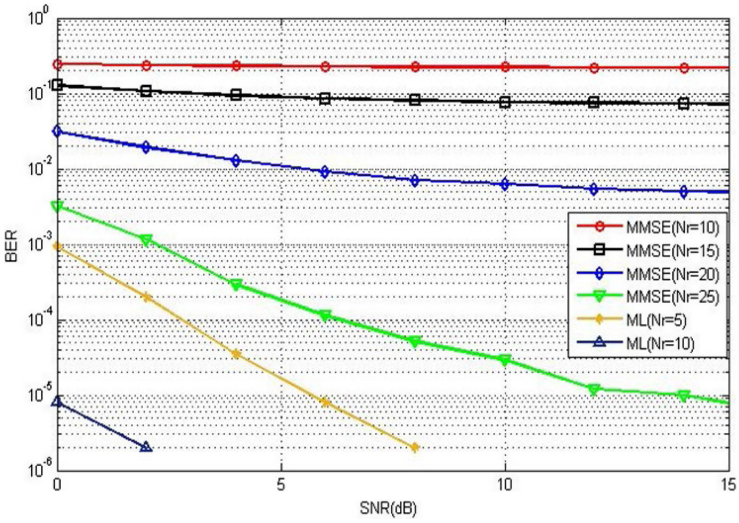

Fig. 9. The BER performance of M-CBPM with MMSE algorithm.

6 Conclusion

Theoretical analysis and simulation results show that our proposed M-CBPM is superior to traditional spatial modulation in term of BER and transmission rate. Moreover, compared with ABPM, this scheme overcomes the defect that the signal can not be received in some zero lobe directions, so it is more suitable for cellular system. It is worth noting that due to the limitation of the number of antennas in current base station, M-CBPM cannot work efficiently. However, with the prevalence of 5G network, more and more base stations will deploy massive MIMO. Then, by virtual of a large number of antennas available, we can choose a smaller $\Delta\omega$ to improve the BER and transmission rate of M-CBPM, and choose a low-complexity algorithm to detect the received signal. Therefore, M-CBPM must have some potential applications in base stations equipped with massive MIMO.

References

1. Lu, L., Li, G.Y., Swindlehurst, A.L., Ashikhmin, A., Zhang, R.: An overview of massive MIMO: benefits and challenges. IEEE J. Sel. Top. Signal Process. **8**(5), 742–758 (2014). https://doi.org/10.1109/JSTSP.2014.2317671
2. Huang, F., Zhan, Y.: Design of spatial constellation for spatial modulation. IEEE Wirel. Commun. Lett. **9**(7), 1097–1100 (2020). https://doi.org/10.1109/LWC.2020.2981612
3. Di Renzo, M., Haas, H., Ghrayeb, A., Sugiura, S., Hanzo, L.: Spatial modulation for generalized MIMO: challenges, opportunities, and implementation. Proc. IEEE **102**(1), 56–103 (2014). https://doi.org/10.1109/JPROC.2013.2287851

4. Wang, J., Jia, S., Song, J.: Generalised spatial modulation system with multiple active transmit antennas and low complexity detection scheme. IEEE Trans. Wirel. Commun. **11**(4), 1605–1615 (2012). https://doi.org/10.1109/TWC.2012.030512.111635
5. Yang, P., Di Renzo, M., Xiao, Y., Li, S., Hanzo, L.: Design guidelines for spatial modulation. IEEE Commun. Surv. Tutor. **17**(1), 6–26 (2015). https://doi.org/10.1109/COMST.2014.2327066
6. Zhao, Y., Hu, J., Xie, A., Yang, K., Wong, K.-K.: Receive spatial modulation aided simultaneous wireless information and power transfer with finite alphabet. IEEE Trans. Wirel. Commun. **19**(12), 8039–8053 (2020). https://doi.org/10.1109/TWC.2020.3019011
7. Ramirez-Gutierrez, R., Zhang, L., Elmirghani, J., Almutairi, A.: Antenna beam pattern modulation for MIMO channels. In: Wireless Communications and Mobile Computing Conference (IWCMC), pp. 591–595 (2012). https://doi.org/10.1109/TWC.2020.3019011
8. Ramirez-Gutierrez, R., Zhang, L., Elmirghani, J.: Antenna beam pattern modulation with lattice reduction aided detection. IEEE Trans. Veh. Technol. **65**, 2007–2015 (2015). https://doi.org/10.1109/TVT.2015.2422299
9. Ghayoula, E., Bouallegue, A., Ghayoula, R., Fattahi, J., Pricop, E., Chouinard, J.-Y.: Radiation pattern synthesis using hybrid Fourier-Woodward-Lawson-neural networks for reliable MIMO antenna systems. In: IEEE International Conference on Systems, Man, and Cybernetics (SMC), Banff, AB, Canada, pp. 3290–3295 (2017). https://doi.org/10.1109/SMC.2017.8123136
10. Lin, Z., Erkip, E., Stefanov, A.: Exact pairwise error probability for the MIMO block fading channel. In: Proceedings of International Symposium on Information Theory and Its Applications (2004)